Scanning Electron Microscopy

Volume 1986
Number 3 *Part III*

Article 12

8-2-1986

Analysis of Voltage-Contrast Decay on Passivated Devices under Electron Beam Probing

Y. Watanabe
Electrical Communication Laboratories

Y. Fukuda
Electrical Communication Laboratories

SCANNING ELECTRON MICROSCOPY/1986/III (Pages 943-948)
SEM Inc., AMF O'Hare (Chicago), IL 60666-0507 USA

0586-5581/86$1.00+05

ANALYSIS OF VOLTAGE-CONTRAST DECAY ON PASSIVATED DEVICES UNDER ELECTRON BEAM PROBING

Y. Watanabe* and Y. Fukuda

Electrical Communication Laboratories, NTT, Tokyo, Japan

(Received for publication February 14, 1986, and in revised form August 02, 1986)

Abstract

Voltage-contrast decay on passivated devices under electron beam probing has been reported. The dependence of the decay time constant of the voltage contrast on the primary electron current, the passivation thickness, and the dielectric constant of the passivation has been analyzed with a recently developed theory of capacitive-coupling voltage contrast. It is found that the theory can be used to estimate the time constant under various observation conditions. Deviation of the time constant from the prediction, depending on the size of the electron beam irradiated area, has been observed and interpreted as being due to secondary electron charging on the surface above the electrode area during electron irradiation of the surrounding surface.

KEY WORDS: Voltage contrast, low accelerating voltage, passivated device, charging phenomenon, local field, electron trajectory, capacitive coupling voltage contrast, decay time constant.

*Address for correspondence:
Electrical Communication Laboratories, NTT,
3-9-11, Midoricho, Musashino-shi, Tokyo 180, Japan.
Phone No: +81-422-59-2678

Introduction

An electron-beam probe using a voltage contrast has been developed and has been applied in logic function tests and fault analysis of LSI devices [1]. In order to avoid radiation damage to internal transistors and the negative charging effect of the passivation surface, the tests have usually been carried out by using low primary electron energies of 1-3 keV [2],[4],[6],[7].

It is well-known that with low accelerating voltages, a voltage-contrast image is visible through the passivation layer for a while after the change in voltages of buried electrodes is finished. However, this contrast fades away with increasing electron irradiation, and finally disappears entirely. This type of contrast is believed to occur because of capacitive coupling of the buried electrodes with the passivation surface. It is called capacitive-coupling voltage contrast (CCVC). As a result of the contrast decay, the observation time is limited and quantitative measurement of the contrast is affected. Thus, it is important to be able to estimate the decay time of CCVC, and recently theoretical models for CCVC have been proposed [3],[8].

In this paper, the dependence of the decay time constant on the primary electron current, the passivation thickness, and the dielectric constant of the passivation is discussed in relation to the proposed model [8]. Secondary electron (SE) charging effects on the surface above the electrode area caused by the electron irradiation on the surrounding surface are discussed with both experimental and the simulated SE trajectories.

The theory of CCVC

A theoretical model for CCVC has been developed and described in detail elsewhere [8]. It adequately explains the variations in CCVC for a passivated device. A brief summary describing the decay time constant of CCVC is as follows.

The model is based on the assumptions that (a) the coefficient δ_{eff} of effective SE collection, meaning the SE detector current I_s / primary electron current I_p, is linearly related to the irradiated-surface potential and (b) (I_s-I_p) is accumulated on the irradiated surface. From these

assumptions, it is shown that the time constant τ_+ when the buried electrode changes from 0 to a positive voltage is given by

$$\tau_+=C_p/(\gamma_+ I_p) \quad (1)$$

where C_p is the capacitance of the passivation layer between the specimen surface and the buried electrode. γ_+ depends on the material of the passivation layer, the accelerating voltage of the primary electron beam, the strength of the extraction field, the geometry of the chamber. and other factors. It is defined by

$$\delta_{eff}=1-\gamma_+(V_{S(t)}-V_{Seq}) \quad (2)$$

with $V_{S(t)}>V_{Seq}$,

where $V_{S(t)}$ is the surface potential. V_{Seq} is the equilibrium potential, where equilibrium is the state in which the incident current is balanced against the emitted current varying due to the irradiated surface potential induced by the accumulated surface charge.

τ_+ can be rewritten as

$$\tau_+=\varepsilon_0/(\gamma_+ d_{eff} J_p) \quad (3)$$

where ε_0 is the dielectric constant of free space and d_{eff} is defined by

$$d_{eff}=d_p/\varepsilon_r. \quad (4)$$

Here, d_p is the passivation layer thickness, ε_r the relative dielectric constant of the passivation, and J_p the current density of the primary electron beam.

Figure 1 shows the relationship between the effective thickness of passivation d_{eff} and J_p with τ_+ as a parameter. Plot represents the value reported by reference [7]. The values of τ_+ estimated from the above results are reasonably close to the previous experimental results.

In the foregoing theoretical description, the influence of secondary electrons emitted from neighboring electrodes at which the potential is different from that of a subject electrode has not been considered. In the following, the dependence of decay time constant on electron beam irradiated area size is described in detail.

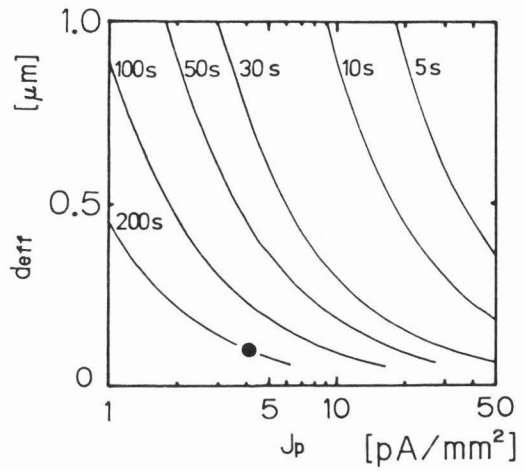

Figure 1. Relationship between effective thickness of passivation d_{eff} and primary electron current density J_p with decay time constant τ_+ of CCVC as a parameter for $\gamma_+=0.10V^{-1}$ [8].

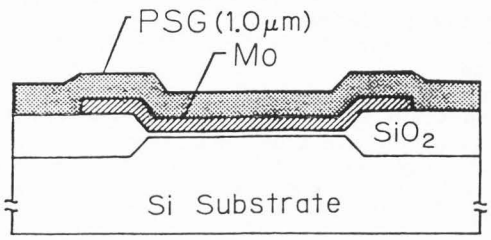

Figure 2. Cross-section of molybdenum MOS capacitor with 1-μm PSG passivation layer.

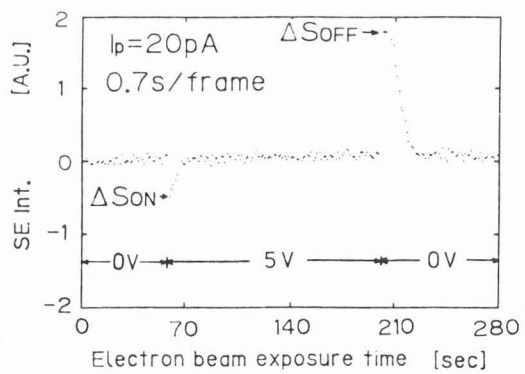

Figure 3. Voltage dependence of SE signal intensity S as a function of electron exposure time.

The dependence of τ_+ on electron beam irradiated area size

The sample is a molybdenum MOS capacitor encapsulated by a phosphosilicate glass (PSG) passivation layer deposited using chemical vapor deposition. Figure 2 shows a cross-section of the specimen. The passivation layer thickness is 1 μm, and the capacitor area 300x300 μm^2.

The dependence of the SE signal intensity on the electrode voltage in the scanning mode was measured, with the measuring point at the central point of the capacitor. The accelerating voltage of the primary electron beam was 2 kV, the beam current 5×10^{-12} to 2×10^{-11} A, and the scanning time per frame 0.7 sec.

A typical result is shown in Fig. 3. When the buried-electrode voltage V_M changes from 0 to 5 V, the SE signal intensity S decreases by ΔS_{ON} and then returns toward the initial value as the number of frames (electron beam exposure time) increases. This is because a negative charge is accumulated on the PSG surface above the electrode. Then, when V_M changes from 5 to 0 V,

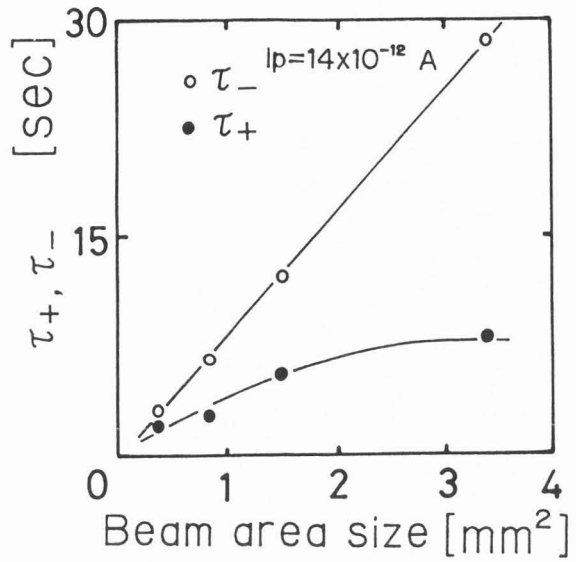

Figure 4. Dependence of $\tau_{\pm}$ on electron beam irradiation area A.

the intensity increases by ΔS_{OFF}, depending on the strength of the surface charge, and decreases toward the initial value as the imaging process continues.

Figure 4 shows the dependence of the measured τ_+ and τ_- on the electron beam irradiated area size, where τ_- denotes the decay time constant of the contrast caused by negative-charge accumulation on the surface. τ_+ and τ_- were respectively calculated by the times when the changes in the SE intensity become $\Delta S_{ON}/e$ and $\Delta S_{OFF}/e$. As I_p is the constant value in these experimental conditions, the beam current density J_p is in reverse proportion to the beam area [7]. Thus, from the relationship given by eq. (3), the theory suggests that both τ_+ and τ_- are in proportion to the beam area. However, as shown in Fig. 4, while the τ_- values are proportional to the beam area, the τ_+ values become non-linearly related as the beam area increases. This result can be explained as follows. Secondary electrons emitted from the surface surrounding the buried electrode are deflected by local fields generated by the potential at the electrode, and a fraction of them are charged on the surface above the electrode. Thus, the τ_+ value is less than the one predicted by the theory.

Charging effects due to electron irradiation in surrounding area

The charging effects due to irradiation at a different point from the electrode area was observed. Figure 5 shows an example of charging of SE emitted from the surface at a different point from the electrode area. This micrograph is of the first frame (7sec/frame) after V_M changed from 5 to 0 V. Electrons had been irradiated at point P in the spot mode for the T_{sp} time under V_M>0V

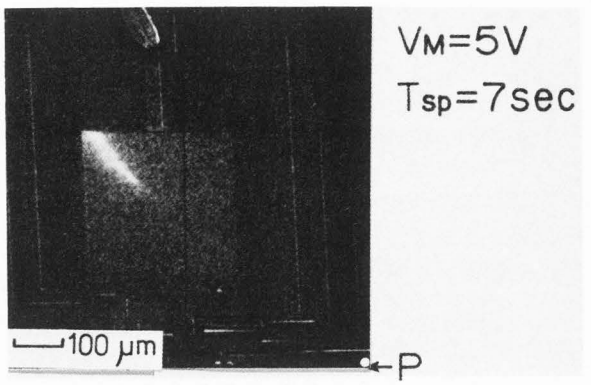

(a)

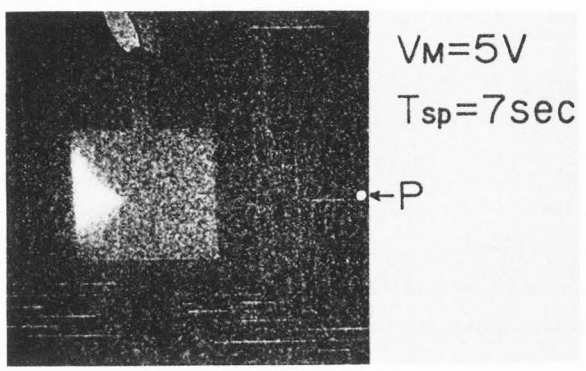

(b)

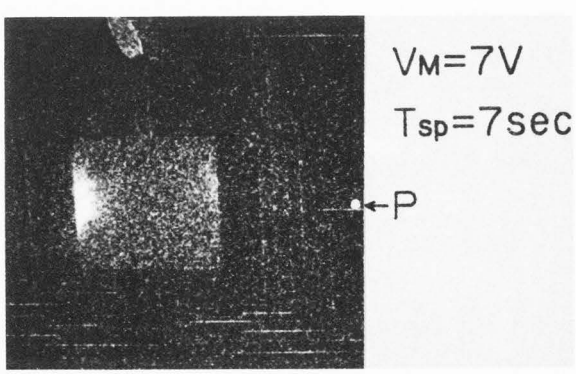

(c)

Figure 5. Secondary electron images indicating charging during spot mode electron irradiation. Electrons were irradiated at point P in the spot mode for T_{sp} under V_M>0 V.

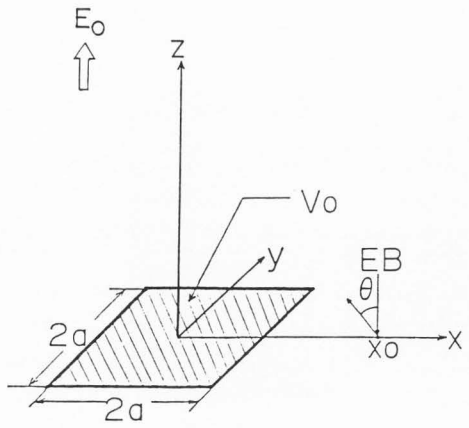

Figure 6. Co-ordinates used to simulate SE trajectory with some parameters.

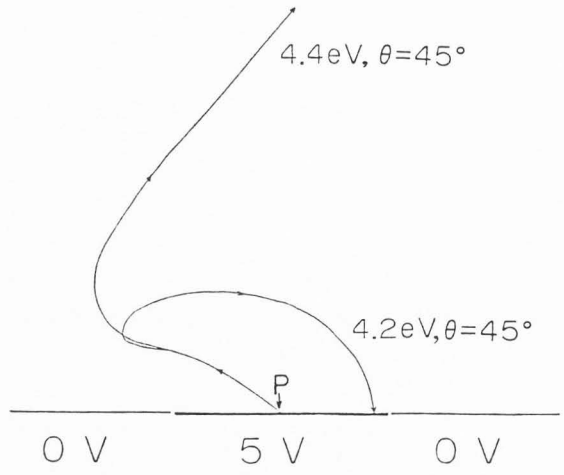

Figure 7. Example of SE trajectories emitted from the surface above the electrode area (X_0=0).

before V_M changed to 0 V. The accelerating voltage of the primary electron beam was 2 kV and the beam current was 5×10^{-12} A. Electron charging is observed as the bright area above the electrode. These results qualitatively agree well with the interpretation of the relationship between τ_+ and the beam area in the preceding section.

In order to confirm the charging mentioned above, two-dimensional simulations of SE trajectories were performed. Figure 6 shows the parameters used in this calculation. The specimen surface boundary is assumed to be infinite, and the extraction field is defined by E_0. The potential distribution above the specimen surface is given analytically as follows:

$$\phi(x,y,z)=E_0\cdot z + \frac{V_0}{2\pi}\left\{\tan^{-1}\left(\frac{(a-x)(a-y)}{z\sqrt{z^2+(a-x)^2+(a-y)^2}}\right) + \tan^{-1}\left(\frac{(a+x)(a-y)}{z\sqrt{z^2+(a+x)^2+(a-y)^2}}\right) + \tan^{-1}\left(\frac{(a-x)(a+y)}{z\sqrt{z^2+(a-x)^2+(a+y)^2}}\right) + \tan^{-1}\left(\frac{(a+x)(a+y)}{z\sqrt{z^2+(a+x)^2+(a+y)^2}}\right)\right\} \quad (5)$$

where it is assumed that the surface potential at the 2ax2a area is V_0 and the one at the other area is 0.

Figure 7 shows some examples of trajectories for a SE ejection angle θ of 45° under the electron irradiated point X_0 of 0. In calculations, the initial velocity in the y-axis direction is assumed to be 0. As shown in Fig. 7, while the electron with an initial energy W of 4.2 eV is deflected back to the specimen, the one with

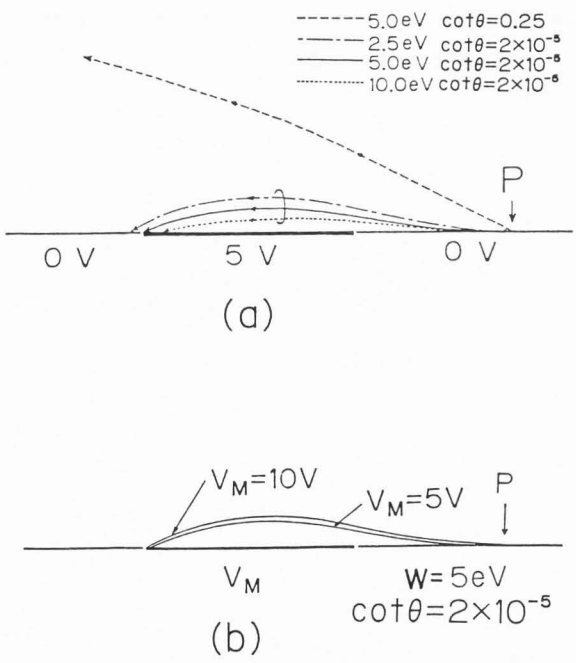

Figure 8. Some examples of SE trajectories under X_0=450 μm.

a W of 4.4 eV is only slightly affected [5].

Figure 8 shows some trajectories under X_0=450μm. Electrons with W higher than 5 eV and cotθ less than 2×10^{-5} reach the surface above the electrode area. This qualitatively agrees well with the experimental results shown in Fig. 5 (b) and (c). Furthermore, as shown in Fig. 8 (b), the dependence of the electron-charging point on the surface potential V_0 explains well the results shown in Fig. 5 (b) and (c).

Conclusion

The voltage-contrast decay phenomena that occur during electron beam testing of passivated LSI devices have been studied. It was shown analytically that a recently developed theory can be used in estimating the order of magnitude of the decay time constant in capacitive-coupling voltage contrast under various observation conditions. In order to obtain good correlation between experiment and theory, it is necessary to determine the values of γ_+ in the respective SEM systems beforehand.

Deviation of the time constant from the predicted values, depending on the size of the electron beam irradiated area, has been observed. This was found to be caused by secondary electron charging on the surface above the electrode area during electron irradiation of the surrounding surface.

Acknowledgement

The authors would like to thank K. Moriya for his continuous encouragement throughout this work.

References

[1] Crichton G, Fazekas P, Wolfgang E. (1980). Electron beam testing of microprocessors. Digest of 1980 IEEE Test Conference. IEEE Computer Soc. Reston, VA, 444-449.

[2] Crosthwait DL, Ivy FW. (1974). Voltage contrast method for semiconductor device failure analysis. Scanning Electron Microsc. 1974: 935-940.

[3] Görlich S, Herrmann KD, Kubalek E. (1984). Basic investigations of capacitive coupling voltage contrast. Microcircuit Engineering, Proc. Int. Enf. Microlithographie, Berlin, Academic Press, London, 451-460.

[4] Kotorman L. (1980). Non-charging electron beam pulse prober on FET wafers. Scanning Electron Microsc. 1980; IV: 77-84.

[5] Nakamae K, Fujioka H, Ura K. (1981). Local field effects on voltage contrast in the scanning electron microscope. J. Phys. D, Appl. Phys., 14 1939-1960.

[6] Nakamae K, Fujioka H, Ura K. (1981). Measurements of internal signal waveforms on passivated MOS LSI using the stroboscopic scanning electron microscope. Trans. Inst. Electron. & Commun. Eng. Jpn. 64C 893-894.

[7] Ura K, Fujioka H, Nakamae K, Ishisaka M. (1982). Stroboscopic observation of passivated microprocessor chips by scanning electron microscopy. Scanning Electron Microsc. 1982; III: 1061-1068.

[8] Watanabe Y, Fukuda Y, Jinno T. (1985). Analysis of capacitive coupling voltage contrast in scanning electron microscopy. Jpn. J. Appl. Phys. 24 1294-1297.

Discussion with Reviewers

K.D. Herrmann: Which is the non-loading E_{PEII} for PSG?

S. Görlich: Capacitive coupling voltage contrast can only be used for low primary electron energies below a typical limiting energy. How is this described in your model? Please, give values for this limiting energy for different passivations?

Authors: CCVC is believed to occur caused by capacitive coupling of the buried electrode to the passivation surface for low primary electron energies (E_{PE}) below E_{PEII}, which is the second crossover potential. We did not measure E_{PEII} for PSG. However, for E_{PE}=2keV no charging was observed, whereas for E_{PE}=3keV negative charging was observed. Therefore, E_{PEII} would take a value in the range of 2 to 3keV. The values of E_{PEII} strongly depend on passivations.

S. Görlich: Your model is based on two assumptions

a) $\delta_{eff}=I_{SE}/I_{PE}=1-\gamma_{\pm}(V_{S(t)}-V_{Seq})$ (6)

and

b) $(I_{SE}-I_{PE})$ charges the surface!

To a): Don't you believe the assumption

$$\delta_{eff}=\delta\int_{eV_B}^{50eV} N_{SE}dE_{SE} \quad (7)$$

is more realistic and physically founded? ($N_{SE}dE_{SE}$=normalized SE spectrum, V_B=potential barrier, which is for low extraction fields $V_B\simeq V_{Seq}+V_{signal}$ and depends on microfield effects, too.)

To b): What about the backscattered electrons?

Authors: a); We agree with your view represented by eq. (6). However, V_B is not constant and depends on some factors such as extraction fields, SE ejection angles as shown in Fig. 7, and others. Therefore, it is difficult to exactly analyze the time dependence of CCVC. We presented a simple phenomenological description of CCVC based on our experimental results (reference [8]).

b); The variation of an irradiated surface potential has to be taken account of the currents of the primary, secondary and backscattered electrons (BE). Although introducing the BE current into our model under the assumption of a constant BE yield as described in reference [3], the time constant τ_+ corresponds to eq. (1). Only the equation representing the equilibrium potential is modified.

K. Ura: I think that γ_+ and γ_- might depend on the voltage pattern beneath the passivation layer in general. Did you measure them as a parameter of linewidth of the pattern?

Authors: We did not measure the dependences of $\gamma_{\pm}$ on the linewidth of the pattern. These values are strongly dependent on the SEM systems. So, by determining these values in the different systems

used beforehand, we could estimate the order of magnitude of the decay time constant for electrodes of various area size.

L. Kotorman: You explain that observed non-linearities occur for τ_+ when scanning large areas, and are caused by SE emitted from neighboring nodes. In principle, this effect appears to be one of the contributors. However, is there any quantitative support of this explanation or could there be other significant causes? What do you think, for example, about the possibility of surface conduction or other sort of charge transfer processes between "non-equipotential domains"? Could it be that with longer time constants these effects merely become more conspicuous?
Authors: Surface conduction and charge transfer processes may contribute to the CCVC decay. However, we think the dominant cause of these effects is charging of SE emitted from neighboring nodes as shown in Fig. 9. Because the non-linearities of τ_+ do not depend on the current density J_p as shown in reference [8], these effects are not related to the value of τ_+, but depend on the rate of the electrode area size to the irradiated one.

L. Kotorman: Did you experiment with other insulators beside PSG? With certain experimental conditions polyimide, for example, accumulates trapped charges that are semi-permanent in nature (depending on beam energy, angle of incidence, current density among other things). These trapped charges become so dominating in the secondary electron generation process that no voltage contrast or CCVC observation is possible. Could it be that you are observing similar phenomenon present on Fig. 5?
Authors: We did not experiment with other insulators. Because the bright area shown in Fig. 5 can easily disappear within a certain time of irradiation, this contrast is not semi-permanent.

L. Kotorman: In eq. 1, the value of γ_+depends on many experimental or given ambient parameters. The combination of these parameters easily can create conditions when no equilibrium states can be obtained within practical limits (similarly to the mentioned trapped charges in polyimide). Although you are mentioning the accelerating voltage range used 1 keV to 3 keV, would you care to put more boundary conditions on these parameters or perhaps comment about their practical ranges.
Authors: Although the γ_+ values depend on many factors, these values would mainly depend on the geometry of the chamber and the strength of the extraction field. Further work is necessary to determine boundary conditions on various ambient parameters.

K.D. Herrmann: How did you calculate the electrical stray field? In this paper E_0 is set to 1 V/mm, although you refer to a value of 4 V/mm (compare your reference [5]). Why didn't you use this value? Does the described effect vanish at higher extraction fields due to the stronger vertical component of the electric field?

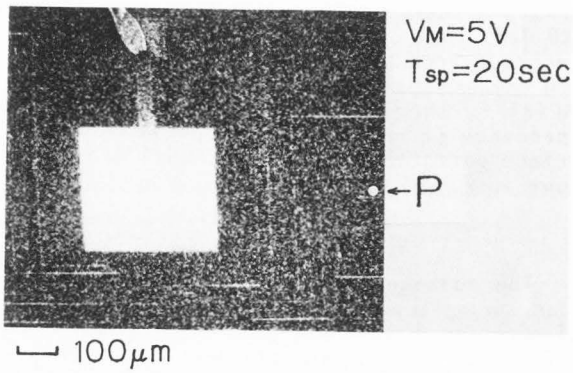

Figure 9. Secondary electron image indicating charging during spot mode electron irradiation. Electrons were irradiated at point P in the spot mode for 20 sec under V_M=5 V.

Authors: We used a conventional Everhart-Thornley detector. According to reference [5], in this type of detector the extraction fields are several volts per millimeter. So, we used 1-5 V/mm in our simulations, and the results qualitatively correspond to the ones shown in Figs. 7 and 8. These figures indicate typical examples of the simulation results.

S. Gorlich: Instead of "observation time" or "decay time constant" the technical term "storage time" should be used, because this was introduced in earlier papers by Ura et al. [7].
Authors: The definition of the term "storage time" introduced by Ura et al. [7] is not clear. From our proposed model it is found that CCVC varies exponentially. We measured directly the time constant.